BIOCHEMISTRY
including biophysical chemistry & molecular biology

Article

pubs.acs.org/biochemistry

Thermodynamics of Binding of Structurally Similar Ligands to Histone Deacetylase 8 Sheds Light on Challenges in the Rational Design of Potent and Isozyme-Selective Inhibitors of the Enzyme

Raushan K. Singh,*[,†] Takayoshi Suzuki,[‡] Tanmay Mandal,[†] Narayanaganesh Balsubramanian,[†] Manas Haldar,[§] Dustin J. Mueller,[†] Jerrod A. Strode,[†] Gregory Cook,[†] Sanku Mallik,[§] and D. K. Srivastava*[,†]

[†]Department of Chemistry and Biochemistry, North Dakota State University, Fargo, North Dakota 58102, United States

[‡]Graduate School of Medical Science, Kyoto Prefectural University of Medicine, Kyoto 603-8334, Japan

[§]Department of Pharmaceutical Sciences, North Dakota State University, Fargo, North Dakota 58102, United States

Supporting Information

ABSTRACT: Among the different histone deacetylase (HDAC) isozymes, HDAC8 is the most highly malleable enzyme, and it exhibits the potential to accommodate structurally diverse ligands (albeit with moderate binding affinities) in its active site pocket. To probe the molecular basis of this feature, we performed detailed thermodynamic studies of the binding of structurally similar ligands, which differed with respect to the "cap", "linker", and "metal-binding" regions of the suberoylanilide hydroxamic acid (SAHA) pharmacophore, to HDAC8. The experimental data revealed that although the enthalpic ($\Delta H°$) and entropic ($\Delta S°$) changes for the binding of individual SAHA analogues to HDAC8 were substantially different, their binding free energies ($\Delta G°$) were markedly similar, conforming to a strong enthalpy−entropy compensation effect. This effect was further observed in the temperature-dependent thermodynamics of binding of all SAHA analogues to the enzyme. Notably, in contrast to other metalloenzymes, our isothermal titration calorimetry experiments (performed in different buffers of varying ionization enthalpies) suggest that depending on the ligand, its zinc-binding group may or may not be deprotonated upon the binding to HDAC8. Furthermore, the heat capacity changes ($\Delta C_p°$) associated with the ligand binding to HDAC8 markedly differed from one SAHA analogue to the other, and such features could primarily be rationalized in light of the dynamic flexibility in the enzyme structure in conjunction with the reorganization of the active site resident water molecules. Arguments are presented that although the binding thermodynamic features described above would facilitate identification of weak to moderately tight-binding HDAC8 inhibitors (by a high-throughput and/or virtual screening of libraries of small molecules), they would pose major challenges for the structure-based rational design of highly potent and isozyme-selective inhibitors of human HDAC8.

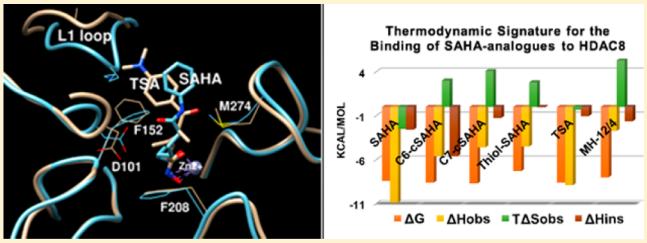

Biophysical and mechanistic studies of enzyme−ligand interactions are routinely pursued to gain molecular insights into the structural−functional features of enzymes.[1] The knowledge gained from such studies is widely utilized in the structure-based rational design of enzyme inhibitors as novel therapeutics.[2] Although the structure-based strategy has been successful with certain enzymes, its widespread utility is often limited because of the inherent structural flexibility of enzymes and proteins.[3,4] Apparently, the "static" structural information obtained from the X-ray crystallographic studies cannot be reliably utilized for the affinity optimization of lead molecules in a drug discovery program.[5,6] Furthermore, the structure-based rational design of the isozyme-selective inhibitor for an enzyme is even more challenging because of the conserved active site pocket shared by its isozymes.

In investigating the structural−functional features of human histone deacetylases (HDACs), we as well as others have realized that among the different HDAC isozymes, HDAC8 is the most highly flexible and/or malleable enzyme, and thereby, it possess the capability of accommodating a wide range of structurally diverse ligands into its active site pocket.[7−9] Notably, unlike the other HDAC isozymes, HDAC8 exhibits weaker binding affinities for all the "pan" (nonspecific) HDAC inhibitors as well as the fluorogenic acetylated peptide substrate.[10−12]

Histone deacetylases (HDACs) are hydrolytic enzymes that catalyze the deacetylation of an acetylated lysine moiety of histones as well as non-histone proteins.[13,14] The human HDAC isozymes are categorized into four major classes based on their phylogeny. Class I HDACs (HDAC1−3 and -8) and class II HDACs (HDAC4, -6, -7, -9, and -10) are metal-

Received: June 7, 2014
Revised: November 16, 2014
Published: November 19, 2014

   dx.doi.org/10.1021/bi500711x | *Biochemistry* 2014, 53, 7445−7458

dependent deacetylases and are inhibited by canonical HDAC inhibitors such as TSA (trichostatin A) and SAHA (suberoylanilide hydroxamic acid).[13,15] In contrast, class III HDACs (sirtuins) are metal-independent enzymes that utilize NAD^+ as a cosubstrate.[16] Class IV HDAC (HDAC11) is phylogenetically unrelated to all the other classes of HDAC.[17]

An aberrant expression of several HDAC isozymes (including HDAC8) has been linked with various pathological conditions, including cancer.[18−22] HDAC8 has been found to be overexpressed in neuroblastoma tumor, which accounts for ∼7% of the total pediatric cancers.[19,20] An inhibition of the catalytic activity of HDAC induces growth arrest and apoptosis in various malignant cells as well as in xenograft mouse models. HDAC inhibitors, namely, SAHA and Romidepsin, have already been approved by the U.S. Food and Drug Administration (FDA) for the treatment of T-cell lymphoma.[23,24] These inhibitors reportedly produce side effects in clinical settings primarily due to the lack of target specificity and/or selectivity. Thus, there has been an ongoing effort to design and/or discover isozyme-selective inhibitors of human HDACs.[24]

X-ray crystallographic studies of ligand−protein interaction have unraveled the mode of binding of an HDAC inhibitor to the enzyme active site pocket.[7−9] On the basis of the structural data of the enzyme−ligand complex, a canonical inhibitor, such as SAHA, has been shown to contain "cap", "linker", and "metal-binding" regions (Figure 1). Notably, the knowledge gained from the structural studies of HDAC8−ligand complexes has been utilized for the structure-based rational design of HDAC8-selective inhibitors by modifying different regions of the SAHA pharmacophore, which has largely been unsuccessful. However, a high-throughput screening of libraries of small molecules has led to the identification of several HDAC8-selective inhibitors, which bear no structural resemblance to a canonical enzyme inhibitor.[25−27]

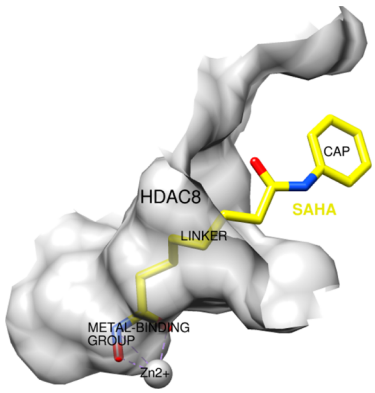

Figure 1. Crystal structure of HDAC8 bound with SAHA (Protein Data Bank entry 1T69) showing the "cap", "linker", and "metal-binding" regions of the ligand. The gray contour represents the inner surface of the enzyme's ligand-binding cavity. This figure was generated using UCSF Chimera (http://www.cgl.ucsf.edu/chimera/).

It has been widely recognized that the therapeutic efficacy of enzyme inhibitors (as potential drugs) in clinical settings is directly related to the thermodynamic (e.g., $\Delta H°$, $\Delta S°$, and $\Delta C_p°$) parameters of the enzyme−inhibitor complexes.[28−31] For instance, the *in vivo* efficacy of the drugs, which interfere with the CD4−gp120 interaction (involved in the HIV infection), has been correlated with the thermodynamic parameters (viz., enthalpy and entropy) of the drug−target complexes.[32] Likewise, the therapeutic efficacy of the HMG−CoA inhibitors (statins) has been positively correlated with their enthalpies of binding to the enzyme.[30] The drug-induced conformational modulation of the target protein dictates the cellular efficacy of the drug, presumably by altering the protein−protein interaction networks associated with various cellular processes.[33]

In view of the facts described above, we purported to investigate the contribution of the different segments of the SAHA pharmacophore (i.e., "cap", "linker", and "metal-binding" regions) in determining the overall thermodynamics of binding of the inhibitor to HDAC8. This was achieved by performing the isothermal titration calorimetry (ITC) studies for the binding of the selected SAHA analogues (Figure 2) that slightly differed with respect to the "cap", "linker", and "metal-binding" regions. We conceived that the knowledge gained from the thermodynamic studies would provide insights into the structure-based rational design of tight-binding and/or isozyme-selective inhibitors for HDAC8. Our experimental data revealed that although the enthalpic and entropic changes for the binding of these SAHA analogues to the enzyme were different, their binding free energies were markedly similar. Furthermore, the magnitudes of the proton inventory, intrinsic enthalpic changes, and heat capacity changes associated with the enzyme−ligand complexes significantly differed from one SAHA analogue to the other, and such differences could not be rationalized in light of the structural differences among the ligands and/or their plausible complexes with the enzyme. Our experimental outcomes presented herein shed light on the potential challenges of structure-based rational design of highly potent and isozyme-selective inhibitors of HDAC8.

MATERIALS AND METHODS

The recombinant form of human HDAC8 was overexpressed and purified from a heterologous host (*Escherichia coli*) using the protocols described previously.[34] All the reagents used in experiments were of analytical grade. Trichostatin A (TSA) was purchased from Sigma. SAHA (suberoylanilide hydroxamic acid) was custom synthesized by Enzo Life Sciences (Plymouth Meeting, PA). Coumarin-SAHA (C6-cSAHA) and thiol-SAHA (t-SAHA) were synthesized in our laboratory as described previously.[34,35]

C7-cSAHA and MH-12/4 were synthesized in our laboratory using the synthetic protocol described below. The synthetic scheme of C7-cSAHA was similar to that of C6-cSAHA[34] except for the use of azelaic acid monomethyl ester in the former case as opposed to suberic acid monomethyl ester in the latter. The physical characteristics and the nuclear magnetic resonance (NMR) data of C7-cSAHA are as follows: $C_{19}H_{24}N_2O_4$; off-white solid; ^{1}H NMR (DMSO-d_6, 400 MHz) δ 1.29 (m, 4H), 1.46−1.51 (q, J = 6.7 Hz, 2H), 1.59 (m, 2H), 1.91−1.95 (t, J = 7.2 Hz, 2H), 2.34−2.37 (t, J = 7.4 Hz, 2H), 2.39 (s, 2H), 6.25 (s, 2H), 7.47−7.49 (d, J = 7.1, 2H), 7.69−7.71 (d, J = 8.6, 2H), 7.77 (s, 2H), 10.48 (s, 1H); ^{13}C NMR (DMSO-d_6, 100 MHz) δ 7.4,14.3, 14.6, 18.0, 21.7, 26.0, 28.4, 94.9, 101.5, 104.2, 104.5, 115.3, 132.2, 142.6, 143.2, 149.5, 158.5, 161.6.

MH-12/4 was synthesized (Scheme 1) using a similar method as described previously.[36] The detail synthetic protocol and the physical characteristics of the intermediates are given below.

dx.doi.org/10.1021/bi500711x | *Biochemistry* 2014, 53, 7445−7458

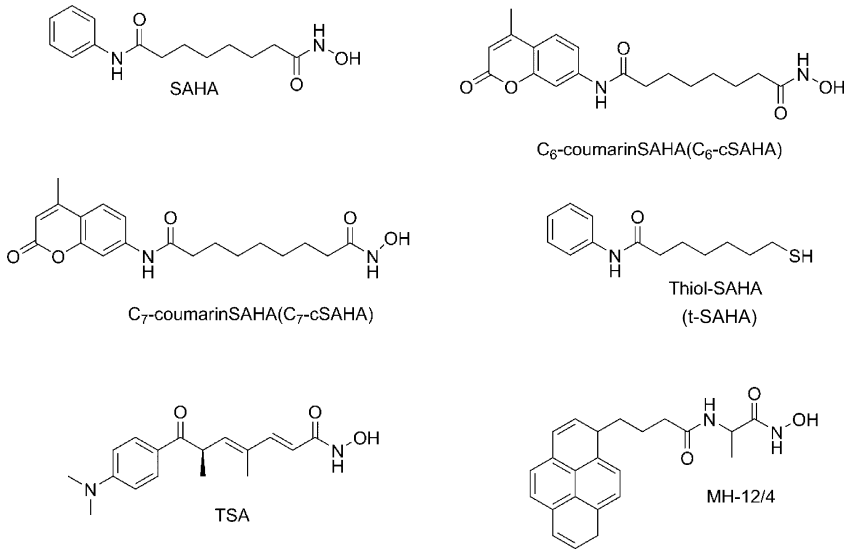

Figure 2. Chemical structures of the SAHA analogues containing different "cap", "linker", and "metal-binding" groups.

Scheme 1. Synthetic Scheme of MH-12/4

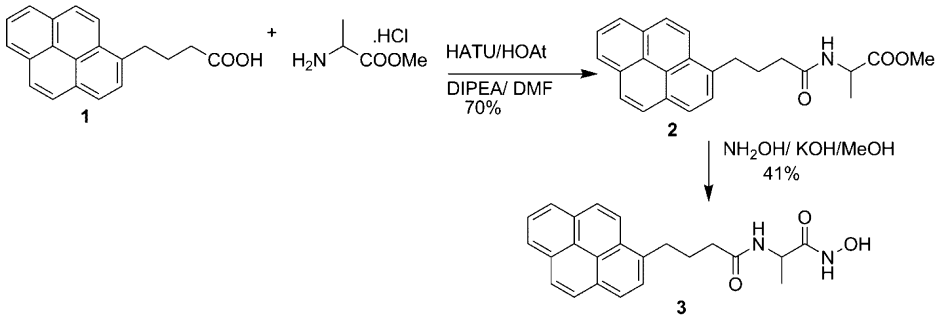

2-(4-Pyren-1-yl-butyrylamino)-propionic Acid Methyl Ester (2). Methyl alanine hydrochloride (279 mg, 2 mmol) was added to a solution of 4-pyren-1-yl-butyric acid (**1**) (576 mg, 2 mmol) prepared in DMF (20 mL). HOAt (272 mg, 2 mmol) and HATU (761 mg, 2 mmol) were added to the reaction mixture, followed by DIPEA (774 mg, 6 mmol). The mixture was stirred overnight under a nitrogen atmosphere at room temperature. The reaction was quenched with brine, and subsequently, DMF was evaporated under reduced pressure. The resulting residue was dissolved in dichloromethane, washed with 10% citric acid, 4% $NaHCO_3$, and brine, and then dried using Na_2SO_4. The solvent was evaporated, and the residue was purified by flash chromatography (R_f = 0.6 in a 3:1 ethyl acetate/hexane mixture) that yielded 521 mg (70% yield) of the pure compound: ^{1}H NMR (DMSO-d_6, 400 MHz) δ 1.20 (d, 3H, J = 8 Hz), 2.01−2.04, (m, 2H), 2.30−2.32 (m, 2H), 3.30−3.33 (m, 2H), 3.70 (s, 3H), 4.20−4.41 (m, 1H), 7.89 (d, 1H, J = 10.4 Hz), 7.99−8.01 (m, 1H), 8.08−8.23 (m, 6H), 8.31 (d, 1H, J = 9.2 Hz), 8.43 (m, 1H).

***N*-(1-Hydroxycarbamoyl-ethyl)-4-pyren-1-yl-butyramide (3).** Compound **2** was reacted with NH_2OH and KOH in methanol. After the reaction, the pH of the reaction medium was adjusted to 3−4 using a solution of 2 N HCl. The reaction mixture was further diluted upon the addition of water, which yielded a white precipitate. The resulting mixture was cooled to 4 °C, and the precipitate was filtered and dried under vacuum to produce the final product: 41% yield; ^{1}H NMR (DMSO-d_6, 400 MHz) δ 1.15 (d, 3H, J = 8 Hz), 1.95−1.97 (m, 2H), 2.24−2.27 (m, 2H), 3.26−3.28 (m, 2H), 4.2−4.23 (m, 1H), 7.95 (d, 1H, J = 6.4 Hz), 8.05−8.08 (m, 2H), 8.11−8.15 (m, 2H), 8.22 (d, 1H, J = 4 Hz), 8.24 (d, 1H, J = 2.8 Hz), 8.26−8.29 (t, 2H, J = 12, 6 Hz), 8.40 (d, 1H, J = 7.6 Hz); ^{13}C NMR (DMSO-d_6, 100.6 MHz) δ 19.11, 28.16, 32.94, 35.41, 46.56, 124.23, 124.82, 124.90, 125.43, 125.59, 126.78, 127.14, 127.87, 128.11, 128.21, 128.82, 129.96, 131.11, 131.55, 137.33, 169.91, 172.28.

Isothermal Titration Calorimetry (ITC) Studies. The thermodynamic parameters for the binding of inhibitors to HDAC8 were determined by isothermal titration calorimetry on a VP-ITC instrument (Microcal Inc., Northampton, MA). All the ITC experiments were performed in at least duplicate or triplicate, and the mean values of the ITC-derived thermodynamic parameters along with the standard deviation are reported in the Results and Discussion. To ensure that the recombinant enzyme expressed and purified in our experimental settings was fully active, we determined its specific activity when it was freshly prepared as well as prior to performing the thermodynamic experiments. For thermodynamic experiments, we used the enzyme that has >90% of its maximal specific activity. For every batch of the enzyme (of highest purity), we performed a control ITC titration experiment with SAHA. Because SAHA invariably gives a stoichiometry of 0.9−1, we calculated the "active site" concentration of the enzyme based on the observed (ITC-derived) stoichiometry of the enzyme−SAHA complex. In most batches of freshly prepared enzyme, the specific activity of the enzyme directly correlated with its "active site" concentration.

dx.doi.org/10.1021/bi500711x | *Biochemistry* 2014, 53, 7445−7458

Hence, we did not have to normalize the enzyme concentration based on the observed stoichiometry of the enzyme−SAHA complex.[37] The observed stoichiometry for the binding of all the ligands was close to 1.

HDAC8 and inhibitor solutions were prepared in a 50 mM Tris/Hepes/triethanolamine/phosphate mixture (pH 7.5) containing 100 mM NaCl and 1 mM TCEP, and they were thoroughly degassed under vacuum. The sample cell of the calorimeter was filled with 1.8 mL (effective volume of 1.4 mL) of 10 μM HDAC8 in a 50 mM Tris/Hepes/triethanolamine/phosphate mixture (pH 7.5) containing 100 mM NaCl and 1 mM TCEP. The enzyme was titrated with 45 aliquots (4 μL each) of 200/400 μM inhibitor (ligand), prepared in the buffers described above. During the course of the titration, the reaction mixture was continuously stirred at 300 rpm. The magnitude of heat produced per injection was calculated by integrating the area under each peak using Origin provided by Microcal. The experimentally observed heat signals were corrected for the background heat signals, which were essentially the heats of dilution of the ligands in the buffer. In most cases, the background signals were comparable to the heat signals obtained at the end of the titration. Hence, the analysis of the ITC data produced similar results whether we subtracted the heat of dilution signals or the residual heat signal (average of five injections) present at the end of the titration (when the enzyme was fully saturated by the ligand). However, to avoid any unforeseen error in the data analysis, we performed the heat of dilution (control titration) experiment with all the ligands utilized herein, and those control experimental data along with the corresponding ITC titration profiles for the binding of different ligands to HDAC8 are shown in the Supporting Information (see Figures S1−S6). The background-subtracted ITC data are presented as the amount of heat produced per mole of the injectant (ligand) as a function of the molar ratio of the ligand to enzyme. To ensure that the enzyme is fully saturated with the ligand (in view of their binding affinities in the micromolar range), we maintained the molar ratio of the ligand to enzyme in the range of 3−5. The experimental data were analyzed using the single-site binding model as described previously by Wiseman et al.,[38] which yielded the magnitudes of the stoichiometry (n), the association constant (K_a), and the standard enthalpy change (ΔH°) for the binding of ligands to HDAC8.

Proton Inventory and Intrinsic Enthalpies for the Binding of Inhibitors to HDAC8. To determine the proton inventory and the intrinsic enthalpic parameters for the binding of the ligands to HDAC8, the ITC experiments were performed in four different buffers, phosphate, Hepes, triethanolamine, and Tris at pH 7.5, which have different ionization enthalpies (ΔH°_{ion}).[39] The magnitude of ΔH°_{obs} obtained from the ITC titration experiments was plotted as a function of the ionization enthalpies (ΔH°_{ion}) of the buffers mentioned above. The data were analyzed by eq 1.

$$\Delta H^\circ_{obs} = \Delta H^\circ_{ins} + p\Delta H^\circ_{ion} \quad (1)$$

where ΔH°_{ins} is the intrinsic enthalpy for the binding of inhibitor to the enzyme, ΔH°_{ion} is the ionization enthalpy of the buffer, and p is the moles of proton released upon binding of inhibitor to HDAC8.

Temperature-Dependent Isothermal Titration Calorimetry (ITC) Studies. To determine the magnitude of heat capacity changes (ΔC_p°) associated with the binding of inhibitors to HDAC8, ITC experiments were performed in the temperature range of 5−25 °C in Tris-HCl buffer, whose ΔC_p° value for the ionization is the lowest among all the buffers mentioned above.[39] HDAC8 was found to be thermally stable in the temperature range described above, which is evident from the temperature-dependent catalytic activity of the enzyme as well as the CD spectra of the protein (data not shown). The ΔC_p° values for the binding of the inhibitors were calculated as the temperature derivatives of the binding enthalpies.

Calculation of Solvent Accessible Surface Areas. The solvent accessible polar and nonpolar surface areas (SAS) of apo-HDAC8 and the HDAC8−inhibitor complexes were determined using GETAREA.[40] The coordinates of apo-HDAC8 [Protein Data Bank (PDB) entry 3F07], HDAC8−TSA (PDB entry 1T64), and HDAC8−SAHA (PDB entry 1T69) complexes were downloaded. The HDAC8 monomers (PDB entry 3F07) containing the bound ligands were separated from the PDB files. The water molecules were manually deleted prior to submitting the PDB files to the GETAREA web service (http://curie.utmb.edu/getarea.html). A default value for the probe radius (1.4 Å) was used for the calculation of solvent water accessible surface areas. The structures of SAHA and TSA were generated using Chem3D (Cambridge Software), and they were converted into Mol2 file format. These Mol2 files were used to determine the solvent accessible surface areas of free inhibitors using MarvinView version 6.1.2 (ChemAxon Ltd.). The changes in solvent accessible surface areas (ΔSAS) upon binding of inhibitors to HADC8 were calculated using the following equation.

$$\Delta SAS = SAS_{HDAC8-inhibitor} - (SAS_{apo\text{-}HDAC8} + SAS_{free\ inhibitor}) \quad (2)$$

Such calculation shows that the binding of SAHA to HDAC8 leads to the burial of 799 and 216 Å^2 of nonpolar and polar solvent accessible surface area (SAS), respectively. The corresponding values for TSA binding were 951 and 131 Å^2, respectively. Hence, the burial of the nonpolar SAS for TSA binding is 152.38 Å^2 higher than that of SAHA. Taking into account the changes in the polar and nonpolar solvent accessible surface areas, we estimated the magnitudes of ΔC_p° as described by Murphy and Freire.[41] The calculated values of ΔC_p° for the binding of TSA and SAHA to HDAC8 were found to be −1.64 and −1.2 kcal mol^{-1} K^{-1}, respectively.

RESULTS

To delineate the thermodynamic contributions for the binding of different regions (viz., "cap", "linker", and "metal-binding") of the SAHA pharmacophore to HDAC8, we selected the following SAHA analogues (Figure 2): (1) the normal SAHA with an anilino group as the "cap", a linear aliphatic C6 as the "linker", and a hydroxamate as the "metal-binding" moiety, (2) C6-coumarin-SAHA (C6-cSAHA), which is similar to SAHA except for the substitution of the anilino moiety in the "cap" region with 7-methyl aminocoumarin, (3) C7-coumarin SAHA (C7-cSAHA), which is similar to C6-cSAHA except for the presence of an additional methylene group in the "linker" region, (4) thiol-SAHA (t-SAHA), which is similar to SAHA except for the substitution of the "metal-binding" hydroxamate group with the thiol moiety, (5) TSA in which the flexible aliphatic C6 "linker" region is replaced by a relatively bulky and constrained hepta-2,4-diene moiety, and (6) MH-12/4 in which the "cap" and the "linker" moieties are replaced by 1,8-

dx.doi.org/10.1021/bi500711x | Biochemistry 2014, 53, 7445−7458

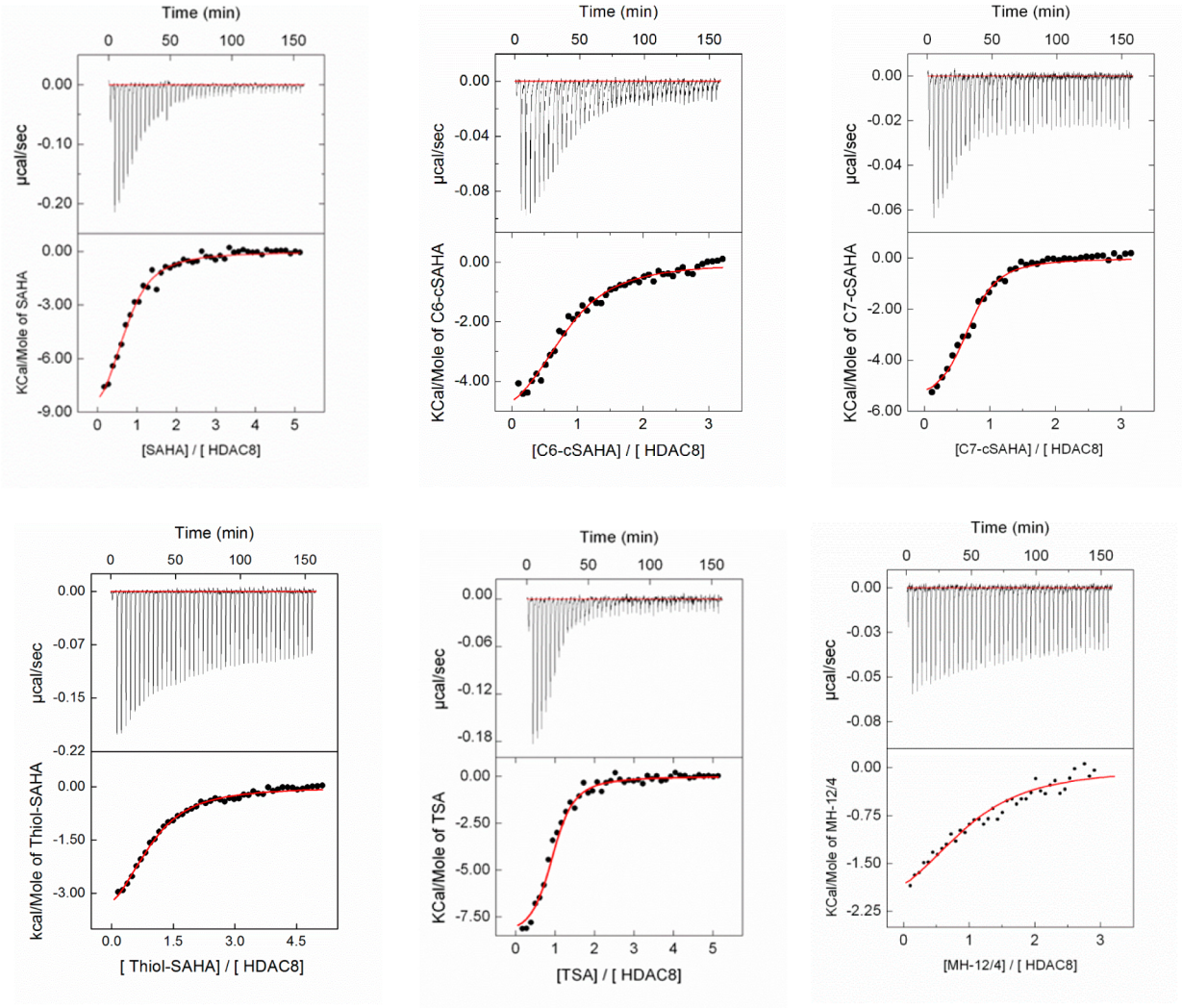

Figure 3. ITC profiles for the binding of the SAHA analogues to HDAC8: SAHA (top left), C6-cSAHA (top middle), C7-cSAHA (top right), t-SAHA (bottom left), TSA (bottom middle), and MH-12/4 (bottom right). The experimental conditions used for the ITC titrations are described in Materials and Methods. The corresponding bottom panels show the plots of the integrated heat signal as a function of the molar ratio of ligand to enzyme. The solid smooth lines in the bottom panels represent the best fits of the data, yielding the observed thermodynamic parameters summarized in Table 1.

Table 1. Summary of the Thermodynamic Parameters for the Binding of SAHA Analogues to HDAC8 in Tris-HCl Buffer (pH 7.5) at 25 °C[a]

ligand	ΔG°_{obs} (kcal/mol)	ΔH°_{obs} (kcal/mol)	$T\Delta S^{\circ}_{obs}$ (kcal/mol)	stoichiometry
SAHA	−8.4 ± 0.3	−10.95 ± 0.5	−2.5 ± 0.2	0.9 ± 0.1
C6-cSAHA	−8.6 ± 0.2	−5.6 ± 0.4	3.0 ± 0.3	0.8 ± 0.2
C7-cSAHA	−8.7 ± 0.1	−4.6 ± 0.5	4.1 ± 0.1	0.8 ± 0.1
t-SAHA	−7.3 ± 0.4	−4.5 ± 0.3	2.8 ± 0.3	1.0 ± 0.1
TSA	−8.6 ± 0.3	−8.93 ± 0.5	−0.3 ± 0.1	0.8 ± 0.1
MH-12/4	−8.0 ± 0.4	−2.72 ± 0.3	5.3 ± 0.4	0.9 ± 0.1

[a]The magnitudes of thermodynamic parameters represent their average values obtained from two or three independent ITC experiments, and the associated standard errors represent the standard deviation from the mean.

dihydropyrene and *N*-(1-oxopropan-2-yl) pentamide moieties, respectively. Using the SAHA analogues mentioned above, we performed the ITC experiments to characterize their binding to HDAC8 as described in Materials and Methods. Figure 3 shows the representative ITC profiles for the binding of SAHA, C6-cSAHA, C7-cSAHA, t-SAHA, TSA, and MH-12/4 to HDAC8 in 50 mM Tris-HCl buffer (pH 7.5) containing 100 mM NaCl and 1 mM TCEP at 25 °C. The top panels of the ITC profiles in Figure 3 show the raw calorimetric data obtained by the titration of 10 μM HDAC8 with 45 injections (4 μL each) of 200/400 μM individual ligands. We performed the control (heat of dilution) experiments for these ligands as described in Materials and Methods (Figures S1−S6 of the Supporting Information). The area under each peak was integrated to obtain the heat signal (kilocalories per mole of injectant) for the formation of the enzyme−ligand complex, and it was

dx.doi.org/10.1021/bi500711x | *Biochemistry* 2014, 53, 7445−7458

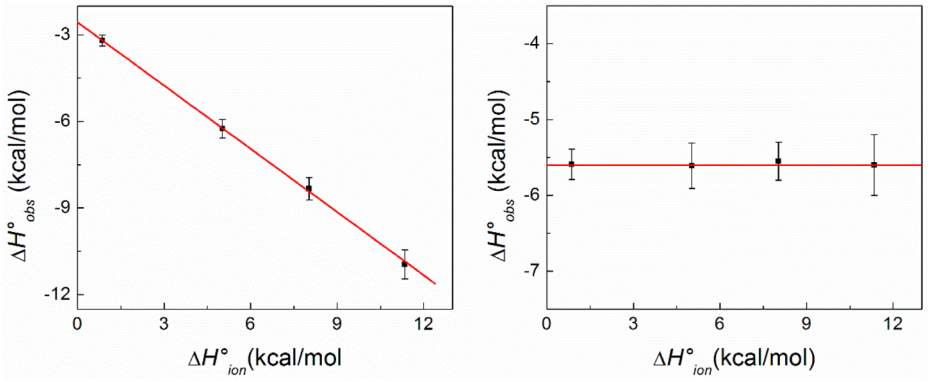

Figure 4. Proton inventory upon the binding of different SAHA analogues to HDAC8. The observed enthalpies ($\Delta H°_{obs}$) for the binding of SAHA (left) and C6-cSAHA (right) to HDAC8 are plotted as a function of the buffer ionization enthalpy ($\Delta H°_{ion}$). The red lines represent the linear regression analyses of the binding data, yielding values of the intrinsic enthalpy and stoichiometry of the proton released to the buffer medium upon the binding of SAHA to HDAC8 of −2.56 ± 0.2 kcal/mol and 0.73 ± 0.04, respectively, and of the binding of C6-cSAHA of −5.6 ± 0.5 kcal/mol and 0.00 ± 0.01, respectively.

corrected for the corresponding heat of dilution (control) signal. The bottom panels of Figure 3 show the resultant (i.e., the experimental minus the control) heat signal plotted as a function of the molar ratio of ligand to enzyme. The experimental data were analyzed using a single-site binding model to obtain the thermodynamic parameters of individual enzyme−ligand complexes (Table1).

A comparative account of the data presented in Table 1 shows several noticeable features. It is evident that all the ligands bind to HDAC8 with a stoichiometry nearly equal to 1. Besides stoichiometry, the data of Table 1 show a marked similarity in the observed free energies ($\Delta G°_{obs}$) for the binding of the SAHA analogues to HDAC8, implying an enthalpy−entropy compensation effect (see Discussion). In rationalizing the structural basis of the thermodynamic parameters listed in Table 1, we noted that the binding enthalpy for t-SAHA was ∼6.4 kcal/mol less favorable than that of SAHA. This difference can be attributed, at least in part, to the monodentate binding of the thiol moiety of t-SAHA to the catalytic Zn^{2+} ion as compared to the bidentate binding mode of the hydroxamate moiety of SAHA. Such a differential mode of binding yields a larger entropic loss in the case of hydroxamate-SAHA over thiol-SAHA (Table 1). In fact, the data of Table 1 reveal that except for SAHA and TSA, all SAHA analogues exhibit a considerable entropic gain upon their binding to HDAC8. Aside from the chelation states, we believe that the differences in the enthalpic and entropic parameters between hydroxamate- and thiol-SAHA are further contributed by the ligand-selective desolvation of the enzyme's active site cavity and/or the conformational flexibility in the enzyme structure (see Discussion). Although a higher magnitude of desolvation of the enzyme's active site pocket upon the binding of t-SAHA (as compared to SAHA) to HDAC8 is supported by the difference in their $\Delta C_p°$ values (see below), a marked difference in the entropic changes in the ligand (due to the monodentate vs bidentate binding modes) weakens such deduction. However, to our surprise, the thermodynamic parameters for the binding of hydroxamate- and thiol-SAHA to HDAC8 showed a remarkable enthalpy−entropy compensation effect, which is manifested in an only 0.9 kcal/mol difference in the standard free energy ($\Delta G°$) change between these ligands (Table 1).

The effect of variation in the "cap" region of the SAHA analogues became evident upon comparison of the thermodynamic parameters for the binding of SAHA and C6-cSAHA (Table 1). The enthalpic change ($\Delta H°$) for the binding of C6-cSAHA to HDAC8 (−5.6 kcal/mol) is ∼5.3 kcal/mol less favorable compared to that with SAHA (−10.9 kcal/mol). On the other hand, the entropic change ($T\Delta S°$) for the binding of the latter ligand (3.0 kcal/mol) is ∼5.5 kcal/mol more favorable compared to that of the former ligand (−2.5 kcal/mol). Hence, once again, a marked enthalpy−entropy compensation effect is noteworthy for the binding of these SAHA analogues to the enzyme, which differ only with respect to the "cap" regions. This feature was further evident upon comparison of the thermodynamic parameters of these ligands with those of MH-12/4, which harbors a bulkier (dihydropyrene) "cap" moiety. While the binding of MH-12/4 to HDAC8 is enthalpically less favorable by 8.2 kcal/mol, it is entropically more favorable by 7.8 kcal/mol compared to that of SAHA. Clearly, the substitution in the "cap" region of the SAHA pharmacophore does not affect the binding free energy ($\Delta G°$) of the ligand to the enzyme, and this feature is accomplished via a compensation between the enthalpic ($\Delta H°$) and entropic ($T\Delta S°$) changes.

A comparison of the thermodynamic parameters for the binding of C6-cSAHA and C7-cSAHA, whose "linker" moieties differ by only one methylene group, reveals the following interesting features. While the enthalpy of binding ($\Delta H°$) of C6-cSAHA to HDAC8 is more favorable by 1.0 kcal/mol compared to that of C7-cSAHA, the corresponding binding entropy is less favorable by 1.1 kcal/mol, resulting in a nearly similar binding free energy ($\Delta G°$). Evidently, strictly from the binding point of view, there is a leeway of changing the "linker" region of the SAHA pharmacophore without gaining or losing the binding free energy.

Unlike SAHA, C6-cSAHA, and thiol-SAHA, which have identical "linker" regions, TSA harbors two unsaturated centers and contains two additional methyl groups, although the latter ligand is one carbon shorter than the other SAHA analogues. A comparative view of the thermodynamic parameters for the binding of SAHA versus TSA (Table 1) reveals that the binding of the latter ligand is enthalpically unfavorable by 2.1 kcal/mol but is entropically favorable by 2.2 kcal/mol, yielding a nearly identical $\Delta G°$ value. A 2 kcal/mol higher favorable binding enthalpy of SAHA compared to that of TSA could be attributed, at least in part, to the fact that the former ligand

dx.doi.org/10.1021/bi500711x | *Biochemistry* 2014, 53, 7445−7458

makes an additional hydrogen bond with the Asp 101 residue of the enzyme, which is evident from the structural data.[7] Apparently, the constraints (imposed by the unsaturated centers) and the bulkiness (due to two methyl groups) in the "linker" region of TSA do not have a significant influence on the binding affinity of the ligand for the enzyme. As will be elaborated in the Discussion, the marked enthalpy−entropy compensation effect observed for the binding of all the SAHA analogues utilized herein, differing with respect to the "cap", "linker", and "metal-binding" regions, could be primarily attributed to the reorganization of water molecules in conjunction with the changes in the conformational flexibility of HDAC8.

Proton Inventory upon Binding of SAHA Analogues to HDAC8. The observed enthalpic changes (ΔH°_{obs}) for the binding of ligands to their cognate enzymes are partially contributed by the enthalpic changes associated with the protonation and/or deprotonation of the ligands and/or enzymes, which can be probed by performing the ITC studies using buffers of varied ionization enthalpies.[42] Because the catalytic Zn^{2+} ion of HDAC serves as a strong Lewis acid, it has the potential to deprotonate the metal-binding groups (e.g., hydroxamate or thiol moieties) of the ligands, resulting in the release of protons. The latter would be absorbed by the buffer anions producing an additional heat signal in the ITC experiments. To quantitate the extent of deprotonation of the metal-binding groups of the SAHA analogues, we performed the ITC studies in four different buffers, namely, phosphate, Hepes, triethanolamine, and Tris (all maintained at pH 7.5), whose ionization enthalpies are known.[39] Figure 4 shows the representative plots for the observed binding enthalpy (ΔH°_{obs}) of SAHA (left panel) and C6-cSAHA (right panel) as a function of ionization enthalpy (ΔH°_{ion}) of the buffers listed above. Note that while the ΔH°_{obs} value for the binding of SAHA to the enzyme is linearly dependent on the ionization enthalpy of the buffers, it remains essentially the same for C6-cSAHA binding. Evidently, despite the structural similarity between SAHA and C6-cSAHA, the binding of the latter ligand to HDAC8 does not release any proton to the exterior medium. The release of the proton in the former case is likely to originate from ionization of the hydroxamate moiety of SAHA upon its binding to the active site resident Zn^{2+} ion, as noted for the binding of other hydroxamate ligands to their cognate metalloenzymes.[43] The solid lines in Figure 4 represent the best linear fits of the experimental data by eq 1 (see Materials and Methods), yielding an intrinsic binding enthalpy (ΔH°_{ins}) and a stoichiometry (p) of the proton released upon the binding of SAHA to HDAC8 of −2.56 ± 0.02 kcal/mol and 0.73 ± 0.4, respectively. The corresponding parameters for C6-cSAHA were −5.6 ± 0.5 kcal/mol and 0, respectively. Note that a part of the observed enthalpy (ΔH°_{obs}) for the binding of SAHA to HDAC8 originates from the deprotonation of its hydroxamate moiety (see Discussion). We performed similar experiments for the binding of C7-cSAHA, thiol-SAHA, TSA, and MH-12/4 in the buffers mentioned above (see Figures S7−S12 of the Supporting Information). All experimental data were analyzed by eq 1, which yielded values of ΔH°_{ins} and stoichiometry (p) of the proton released upon enzyme−ligand interaction (Table 2). A close examination of the data of Tables 1 and 2 reveals that depending on the chemical structure of the SAHA analogue, the intrinsic binding enthalpy (ΔH°_{ins}) is lower (e.g., in the case of SAHA, t-SAHA, TSA, and C7-cSAHA) than the observed binding enthalpy (ΔH°_{obs}) or the parameters listed above are nearly identical (e.g., in the case of C6-cSAHA and MH-12/4).

Table 2. Summary of the Intrinsic Thermodynamic Parameters for the Binding of SAHA Analogues to HDAC8

ligand	ΔH°_{ins} (kcal/mol)	stoichiometry of proton released to buffer (p)
SAHA	−2.56 ± 0.2	0.73 ± 0.4
C6-cSAHA	−5.6 ± 0.5	0.00 ± 0.01
C7-cSAHA	−1.24 ± 0.21	0.31 ± 0.03
t-SAHA	−0.06 ± 0.1	0.39 ± 0.02
TSA	−1.04 ± 0.31	0.71 ± 0.04
MH-12/4	−1.63 ± 0.20	0.08 ± 0.03

With regard to the magnitude of proton release (Table 2), we note that there is no net proton release upon binding of C6-cSAHA to HDAC8, and there is a miniscule amount of proton release (0.08) upon binding of MH-12/4 to the enzyme. To our surprise, the stoichiometry of proton release increased from 0 to 0.31 with an increase in the "linker" length of the ligand by one methylene group (i.e., from C6- to C7-cSAHA), which is reflected in the difference between the ΔH°_{ins} and ΔH°_{obs} values of C7-cSAHA. Hence, it appears that the increase in the "linker" chain length (even by one carbon chain) alters the mode of binding of C7-cSAHA to HDAC8 such that the hydroxamate moiety of the ligand resides in the proximity of the active site resident Zn^{2+} ion, resulting in its deprotonation. Hence, the most interesting observation from the proton inventory data is that although the metal-binding moiety (hydroxamate) of the SAHA analogues (SAHA, TSA, C6-cSAHA, C7-cSAHA, and MH-12/4) remains the same, the magnitude of deprotonation is dependent on the type of "linker" and "cap" regions, and this feature is intrinsic to their modes of binding to HDAC8 (see Discussion).

We note that among SAHA analogues, which release protons to the exterior buffer medium, the stoichiometry (p) of proton release varies from one ligand to the other, and such a difference can be ascribed to the differential influence of the enzyme's active site Zn^{2+} ion in modulating the pK_a values of the metal-binding moieties of the ligands. Using the Henderson−Hasselbalch equation, we could predict the pK_a values of the hydroxamate moieties of TSA and SAHA bound to HDAC8 as being equal to 7.0 and 7.1, respectively, and that for the thiol moiety of t-SAHA as being 7.7. Given that the pK_a values of hydroxamate and thiol moieties in aqueous solution are 8.9 and 10.2, respectively,[44,45] it appears logical to surmise that the active site resident Zn^{2+} ion (serving as a Lewis acid) decreases their pK_a values. Consequently, the hydroxamate and thiol groups of the ligands described above preferentially interact with the active site resident Zn^{2+} ion in their deprotonated forms at pH 7.5. On the other hand, because the proton inventory for the binding of C6-cSAHA and MH-12/4 is equal to zero (or nearly zero), it appears evident that the hydroxamate moieties of the latter ligands are not deprotonated while they are bound to the enzyme's active site pocket. This feature could be attributed, at least in part, to differential positioning of the hydroxamate moieties of C6-cSAHA and MH-12/4 proximal to the Zn^{2+} ion, in comparison to TSA, SAHA, and the other ligands. In this regard, it should be mentioned that independent computational studies by Wu et al. and Chen et al. provide contradictory results with regard to the change in the protonation state of the hydroxamate

dx.doi.org/10.1021/bi500711x | Biochemistry 2014, 53, 7445−7458

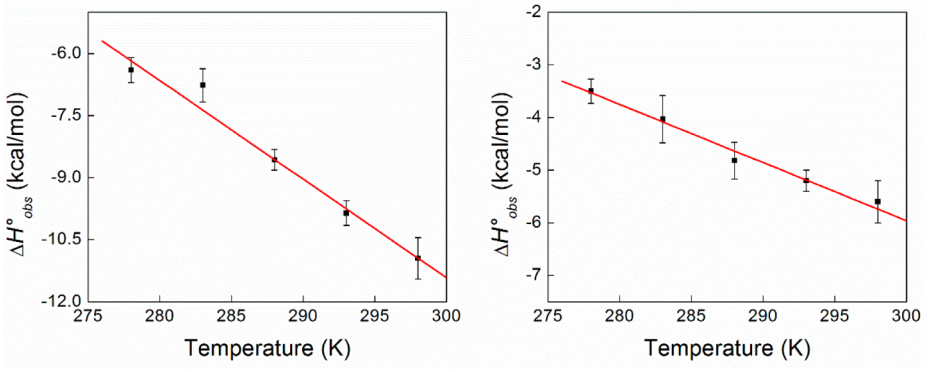

Figure 5. Temperature dependence of the observed enthalpy (ΔH°_{obs}) for the binding of SAHA (left) and C6-cSAHA (right) to HDAC8. The ΔH°_{obs} values are plotted as a function of temperature. The red lines represent the linear regression analysis of the data, yielding values of ΔC_p° for binding of SAHA and C6-cSAHA to HDAC8 of -0.23 ± 0.02 and -0.11 ± 0.01 kcal mol^{-1} K^{-1}, respectively.

moiety of SAHA analogues upon binding to HDAC8 (see Discussion).[46,47]

The intrinsic enthalpy (ΔH°_{ins}) for protein−ligand interaction, derived from the proton inventory data, provides the magnitude of binding enthalpy in the absence of the heat signal (due to protonation and/or deprotonation) contributed by the buffer medium. Hence, the intrinsic enthalpic changes are generally taken as the measures of the binding enthalpies, originating from the direct (noncovalent) interactions between the ligands and their cognate proteins. A comparative account of the intrinsic enthalpy for the binding of the different SAHA analogues to the enzyme (Table 2) suggests that their values are markedly different from one another, and such differences could primarily arise from the reorganization of the water molecules in conjunction with the differential modulation in the dynamic features of the enzyme (see Discussion).

Temperature Dependence of Thermodynamic Parameters of Enzyme−Ligand Interactions. To gain insight into the molecular forces involved in the binding of the SAHA analogues to HDAC8, we determined the heat capacity changes (ΔC_p°) associated with the enzyme−ligand interactions by performing the ITC experiments in the temperature range of 5−25 °C. We performed all the temperature-dependent ITC experiments in Tris-HCl buffer, as the ΔC_p° for the ionization of this buffer has the lowest value.[39] Figure 5 shows the representative ΔC_p° plots for the binding of SAHA (left panel) and C6-cSAHA (right panel) to HDAC8. Note that the observed enthalpy (ΔH°_{obs}) for the binding of both these ligands to HDAC8 becomes more favorable (i.e., its negative value increases) with an increase in temperature. The solid lines in Figure 5 represent the linear regression analysis of the experimental data, yielding ΔC_p° values for the binding of SAHA and C6-CSAHA of -0.23 ± 0.02 and -0.11 ± 0.01 kcal mol^{-1} K^{-1}, respectively. We performed similar temperature-dependent ITC experiments for the binding of other SAHA analogues to HDAC8 (see Figures S13−S18 of the Supporting Information), and their ΔC_p° values are summarized in Table 3. Note that the ΔC_p° values for the binding of all SAHA analogues to HDAC8 are negative, but their magnitudes are significantly different. According to the classical model of protein folding and unfolding as well as protein−ligand interactions, a negative value of ΔC_p° primarily arises due to hydrophobic interactions.[48−50] As per this model, thiol-SAHA ($\Delta C_p^{\circ} = -0.27$ kcal mol^{-1} K^{-1}) and C7-cSAHA ($\Delta C_p^{\circ} = -0.05$ kcal mol^{-1} K^{-1}) should make the most and least hydrophobic interactions within the ligand-binding cavity of HDAC8,

Table 3. Summary of the Heat Capacity Changes Associated with the Binding of SAHA Analogues to HDAC8

ligand	ΔC_p° (kcal mol^{-1} K^{-1})	temp (K), where $\Delta G^{\circ} = \Delta H^{\circ}$
SAHA	-0.23 ± 0.02	288
C6-cSAHA	-0.11 ± 0.01	329
C7-cSAHA	-0.05 ± 0.02	377
t-SAHA	-0.27 ± 0.01	310
TSA	-0.21 ± 0.01	295
MH-12/4	-0.13 ± 0.02	341

respectively. This is unlikely to be the case, because the polar and nonpolar surface areas in these ligands are not too different. Hence, as noted with many enzyme-ligand complexes, the ΔC_p° values for the binding of the SAHA analogues to HDAC8 cannot be rationalized solely in light of the classical hydrophobic model (see Discussion).[51] This is further substantiated by the fact that the ΔC_p° values, calculated on the basis of the changes in the water accessible surface areas of the enzyme (Materials and Methods), for the binding of TSA and SAHA to HDAC8 are ∼1 order of magnitude higher (more negative) than the experimentally determined values (Table 3).

The temperature-dependent ITC data for the binding of ligands to HDAC8 allowed us to ascertain a plausible enthalpy−entropy compensation effect, which is the hallmark feature of the biomolecular interactions. The molecular origin of such a compensatory effect often lies in the weak physical interactions and/or the direct involvement of water molecules in the binding processes.[52−55] To probe the enthalpy−entropy compensation effect for the binding of the SAHA analogues to HDAC8, we plotted the experimentally determined values of ΔH° and ΔG° as a function of $T\Delta S^{\circ}$. Figure 6 shows representative enthalpy−entropy compensation plots for the binding of SAHA (left panel) and C6-cSAHA (right panel) to HDAC8. Note that whereas the ΔH° value linearly increases as a function $T\Delta S^{\circ}$, the value of ΔG° remains nearly invariant for the binding of the ligands to the enzyme. As a consequence, both these plots intersect at a common point at which the magnitude of $T\Delta S^{\circ}$ is equal to zero. When $T\Delta S^{\circ} = 0$, ΔG° can be envisaged to be solely contributed by ΔH°. We determined the temperatures at which ΔH° is equal to ΔG° (by interpolating the parameters described above from the corresponding ΔC_p° plots), and they were found to be 288 and 329 K for the binding of SAHA and C6-cSAHA, respectively. We performed a similar ITC titration and data analysis for the temperature-dependent binding of other SAHA

dx.doi.org/10.1021/bi500711x | Biochemistry 2014, 53, 7445−7458

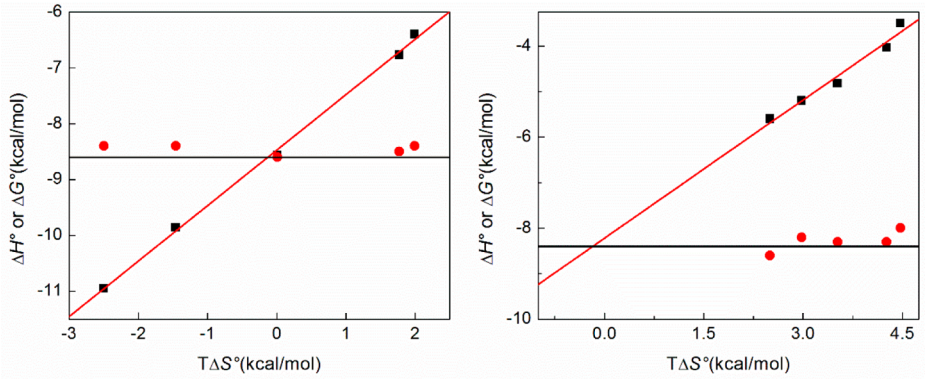

Figure 6. Enthalpy−entropy compensation plot for the binding of SAHA (left) and C6-cSAHA (right) to HDAC8. The values of ΔH° (black squares) and ΔG°_{obs} (red circles) were plotted as a function of $T\Delta S^\circ$. Note that the value of ΔG° essentially remain the same because of the enthalpy−entropy compensation.

analogues to HDAC8 (see Figures S19−S21 of the Supporting Information) and determined the temperatures at which ΔH° is equal to $T\Delta S^\circ$ (summarized in Table 3). Evidently, the enthalpy−entropy compensation temperature varies from one SAHA analogue to the other, and the highest and the lowest temperatures were observed for the binding of C7-cSAHA (377 K) and SAHA (288 K), respectively. Notably, the range of the enthalpy−entropy compensation temperature observed for the binding of the SAHA analogues utilized herein is higher than those (between 250 and 315 K) previously reported by Lumry and Rajender for diverse bimolecular/physical interactions.[53] We believe that the origin of our observed difference in the ligand specific compensatory effects lies in the favorable (i.e., vibrational and hydrophobic entropies) and unfavorable (i.e., rotational, translational, and conformational) entropies of the interacting species (which are offset by the complementary enthalpic changes). Such a feature could arise, at least in part, from the ligand-induced modulation in the protein dynamics and/or flexibility and/or the reorganization of solvent (water) on the surface of ligand as well as the ligand-binding cavity upon the formation of the ligand−protein complexes.

DISCUSSION

We provide, for the first time, a detailed account of the thermodynamic data for the binding of structurally similar SAHA analogues to HDAC8. This paper elaborates on the contribution of different, viz., "cap", "linker", and "metal-binding", regions of the SAHA pharmacophore to the modulation of the thermodynamic parameters of the enzyme−ligand complexes. We argue that the difference in thermodynamic parameters for the binding of the SAHA analogues to HDAC8 can be attributed to the reorganization of water molecules on the surface of the ligands and/or enzyme ligand-binding cavity, as well as to the inherent conformational flexibility and/or dynamics in the protein structure.

The experimental data presented herein lead to the following conclusions. (1) Although the enthalpic (ΔH°) and entropic ($T\Delta S^\circ$) contributions for the binding of the different SAHA analogues—with varying "cap", "linker", and "metal-binding" regions—to HDAC8 are markedly different, their standard free energy changes (ΔG°) are nearly identical among hydroxamate-containing ligands, and they are slightly more favorable (by ∼1.3 kcal/mol) than the binding free energy of a thiol-containing ligand (t-SAHA), resulting in a high degree of enthalpy−entropy compensation among different SAHA analogues (Table 1 and Figure 7). (2) The enthalpy−entropy compensation effect also accounts for the changes in the

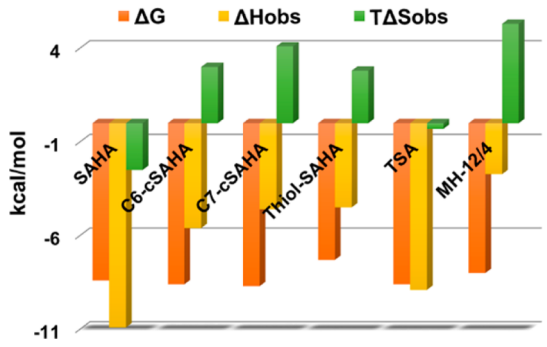

Figure 7. Thermodynamic signatures for the binding of the different SAHA analogues to HDAC8. Despite the marked differences in the binding thermodynamic signatures of these ligands, their binding free energies are nearly the same, highlighting an enthalpy−entropy compensation effect.

temperature dependence in the parameters of binding of SAHA analogues to HDAC8 (Figure 6 and Figures S19−S21 of the Supporting Information). (3) Except for C6-cSAHA and MH-12/4, the binding of other SAHA analogues to HDAC8 results in the release of proton to the exterior medium, and the stoichiometry (p) of proton release is dependent on the changes in the pK_a values of their metal-binding groups under the influence of the catalytic Zn^{2+} ion (serving as a Lewis acid) of the enzyme (Table 2). (4) The heat capacity changes (ΔC_p°) associated with the binding of the different SAHA analogues to HDAC8 cannot be rationalized in view of the classical hydrophobic binding model of the enzyme−ligand complexes. In the case of SAHA and TSA, whose crystal structures in complex with HDAC8 are known, the experimentally determined ΔC_p° values differ by one order magnitude from those calculated on the basis of the changes in the water accessible surface areas of the enzyme and the ligands.

Because the HDAC-catalyzed reaction involves deacetylation of acetylated lysine residues of peptide substrates, it is not surprising to see that the enzyme is poised to accommodate the aliphatic side chain of the lysine residue. Recent proteomic studies have shown that for an artificial peptide to be utilized as an HDAC8 substrate, it must harbor an aromatic amino acid at the C-terminal end of the acetyllysine residue.[56] In such substrate, the acetyl moiety interacts with the active site

dx.doi.org/10.1021/bi500711x | Biochemistry 2014, 53, 7445−7458

resident Zn^{2+} ion, the aliphatic side chain of the lysine moiety sits in the tubular binding cavity, and the aromatic side chain of the C-terminal (aromatic) amino acid occupies the enzyme's entry pocket. In view of these features, it is not surprising that SAHA (harboring the corresponding "metal-binding", "linker", and "cap" regions) serves as a structural analogue of the substrate and thus inhibits enzyme catalysis. However, unlike other HDAC isozymes, HDAC8 is known to interact with structurally diverse ligands, and therefore, the latter must possess a conformationally flexible binding cavity to accommodate non-SAHA pharmacophores (e.g., SB-379278A, CRA-A, and other "linkerless" inhibitors) with reasonable binding affinities.[25−27] In this regard, HDAC8 falls in the category of promiscuous enzymes, which are usually flexible in nature, and they do not interact strongly with their cognate ligands.[57−59] A survey of the binding affinities of substrates and inhibitors with class I HDACs reveals that HDAC8 indeed has the weakest binding affinity for its substrates and inhibitors (see below).[10−12] Moreover, the X-ray crystallographic data reveal that HDAC8 attains significantly different conformations even to accommodate structurally similar ligands (e.g., SAHA and TSA), highlighting the intrinsic flexibility of the enzyme's active site pocket (Figure 8).[7]

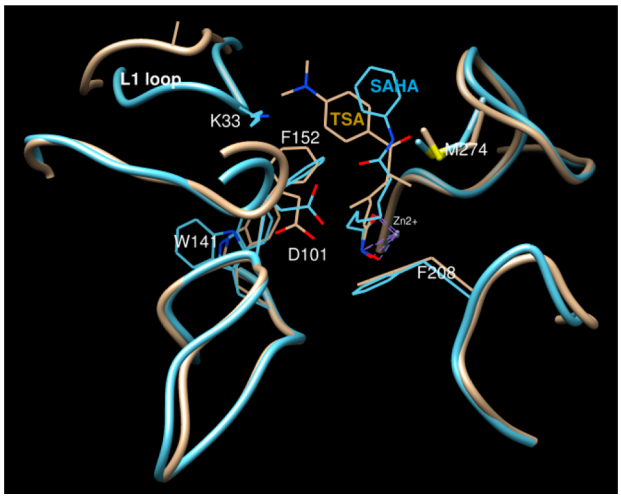

Figure 8. Topologies of the enzyme active site's pocket forming loops (and the residues therein) in different HDAC8−ligand complexes. This figure was generated using UCSF Chimera (http://www.cgl.ucsf.edu/chimera/).

An enzyme−substrate/inhibitor interaction involves "multipoint" contacts between the juxtaposed atoms of the interacting species, and the overall binding energy of an enzyme−ligand complex is derived from the cumulative sum of the energies contributed by the individual interacting atoms.[60,61] As discussed below, the latter may have both "positive" and "negative" cooperative manifestations.[60] Hence, the different binding regions (viz., "cap", "linker", and "metal-binding" group) of a SAHA analogue can be envisaged to contribute synergistically to the overall binding energy of the ligand. Because the different binding region of a SAHA analogue may interact differently within the enzyme's active site pocket, one would predict that the binding free energies of various SAHA analogues would be substantially different (see Table 1). However, to our surprise, the binding free energies of different SAHA analogues with HDAC8 are similar (7.3−8.6 kcal/mol). We note that besides the ligands used herein, other SAHA analogues also show similar binding free energies. For example, Bradner and co-workers have reported the K_i values of several inhibitors, of which at least three inhibitors, viz., APHA, pyroxamide, and 4-PBHA, are the structural analogues of SAHA, for HDAC8.[10] The corresponding K_i values of these inhibitors for HDAC8 have been reported to be 0.6, 1.0, and 1.85 μM, which could be translated into binding free energies of −8.4, −8.1, and −7.8 kcal/mol, respectively. Note that these values are very similar to the binding free energies of the SAHA analogues described herein (Table 1). Taken together, HDAC8 exhibits the potential to interact with structurally diverse SAHA analogues with similar binding free energies (see below).

Our proton inventory data provide evidence that depending on the chemical structures of the SAHA analogues, HDAC8 exhibits the potential to extract different magnitudes of binding energy from the different regions of the ligands. The catalytic divalent metal ions (e.g., Zn^{2+}) in various metallohydrolases function as Lewis acids, and they generate tightly bound OH^- ion (by deprotonating water), which serves as a strong nucleophile during the hydrolytic reactions.[62,63] By virtue of this feature, the HDAC8-bound Zn^{2+} ion is expected to deprotonate the metal-binding groups (e.g., hydroxamate and thiol) and subsequently interact with their anionic forms. Notably, a recent quantum mechanics study performed by Chen. et al. also suggests that the hydroxamate moieties of SAHA and TSA are deprotonated upon binding of Zn^{2+} to HDAC8.[47] Unlike the computational study described above, in which the hydroxamate moieties of ligands are predicted to be equally deprotonated upon their binding to HDAC8, our ITC experiments demonstrate that the extents of deprotonation of the zinc-binding groups of the ligands (upon binding to the enzyme) are remarkably different from one another (Table 2). Because the active site pocket of HDAC8 is relatively hydrophobic (Figure 9), we believe the difference in the

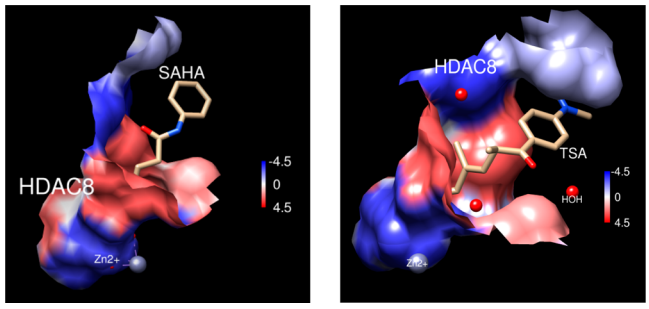

Figure 9. Surface representation of the HDAC8−ligand complexes showing the differences in surface topology, shape, and organization of crystallographically captured water molecules. The residues located in a 5 Å zone around the ligand (TSA/SAHA) are shown, and they are colored according to their hydrophobicity index. The crystallographically captured water molecules present on the surface of the binding cavity are shown as red spheres.

proton inventory of the SAHA analogues is a consequence of the Zn^{2+}-mediated perturbation of the pK_a values of the metal-binding groups, and the extent of such perturbation is dictated by the distance between the Zn^{2+} and the ionizable metal-binding groups. We argue that the other regions (e.g., "cap" and "linker") of the ligands are intimately involved in positioning of the metal-binding groups proximal to the active site resident Zn^{2+} ion. Whether the proton released from the Zn^{2+}-binding

dx.doi.org/10.1021/bi500711x | Biochemistry 2014, 53, 7445−7458

moieties of our ligands is directly released to the exterior buffer media or is shuttled via the enzyme's active site resident His142 is not clear at this time.[47]

The question of why some of the SAHA analogues, particularly C6-cSAHA (and to some extent MH-12/4), do not release any proton upon binding to HDAC8 arises. The only major difference between C6-cSAHA and SAHA is that the former ligand contains a bulkier coumarin (instead of aniline) moiety in the "cap" region. A similar situation exists in the case of MH-12/4, which contains a bulky pyrene moiety in the "cap" region. Hence, it appears plausible that the bulkier "cap" moieties (present in both C6-cSAHA and MH-2/14) preclude the positioning of their terminal hydroxamate moieties proximal to the active site Zn^{2+} ion; thus, they are not effectively deprotonated. However, this simplistic explanation does not hold in the case of C7-cSAHA [showing a proton inventory of 0.31 (see Table 2)], which also contains coumarin as the "cap" moiety but slightly differs from C6-cSAHA because of the presence of an additional methylene group in the "linker" region. Hence, both the "cap" and "linker" regions of the SAHA analogues modulate the avidity of their metal-binding moieties (e.g., hydroxamate) to the catalytic Zn^{2+} ion. Furthermore, depending on the extent of ionization of the metal-binding groups, the gain in favorable binding free energy, originating from the electrostatic interaction between the catalytic Zn^{2+} ion and the anionic form of the metal-binding group, of the different SAHA analogues is likely to be different. In view of the facts presented above, we surmise that depending on the chemical structure of the SAHA analogue, the enzyme extracts a different magnitude of binding energy from different regions of the ligand structure. Additionally, because the ligand-binding cavity of HDAC8 is comprised of several pocket-forming loops whose orientations are differently modulated even upon the binding of structurally similar ligands (Figure 8),[7] it is likely that the metal-binding groups of the SAHA analogues may experience a substantially different microenvironment within the enzyme's binding pocket, leading to their differential deprotonation.

The thermodynamics of binding of the SAHA analogues to HDAC8 described in this work clearly shows a strong enthalpy−entropy compensation effect, which is a fairly common phenomenon in a variety of biomolecular interactions. Apart from biomolecular interactions, enthalpy−entropy compensation has been observed in a wide variety of other physiochemical phenomena in water, such as solvation of ions, ionization of electrolytes, hydrolysis, oxidation reduction, quenching of indole fluorescence, etc.[53] In protein chemistry, the enthalpy−entropy compensation effect has been frequently observed in the temperature-dependent binding of ligands to their cognate proteins.[54,64,65] The enthalpy−entropy compensation effect has been widely observed in the binding of structurally similar ligands to their common target, and this feature is known to hinder the affinity optimization of lead molecules toward finding a tight-binding drug molecule.[66] Aside from equilibrium binding, the enthalpy−entropy compensation has been reported in various kinetic processes, including the transient kinetics for the binding of SAHA and TSA to HDAC8 reported previously from our laboratory.[67,68] However, the enthalpy−entropy compensation effect is not observed in processes that involve stronger interactions.[52,69,70] Taken together, the enthalpy−entropy compensation effect appears to be a ubiquitous phenomenon involving weak interactions among biomolecular species in aqueous solution.[52,53,71]

The physical origin of enthalpy−entropy compensation has been a matter of significant controversy. This is partly because the molecular origin of the hydrophobic effect, initially proposed by Kauzman and Tanford, is not universally applicable, and it appears that depending on the molecular context, the hydrophobic effect is either enthalpically or entropically dominated.[72,73] In recent years, the molecular explanation for the origin of enthalpy−entropy compensation effect has been revised.[52,53,70−77] In the case of binding of structurally similar ligands to their target, an entropic penalty, caused by a decrease in the flexibility and/or randomness of the ligand and/or the protein upon ligand−protein interaction, is often compensated by the enthalpic gain due to atomic contacts, producing the enthalpy−entropy compensation effect.[74] Qian has demonstrated that the local changes in the conformational fluctuations of a protein upon binding to its ligand are transmitted to the rest of the protein, and the enthalpy and the entropy associated with these conformational fluctuations compensate each other.[75] In addition, the reorganization of water molecules surrounding the ligands as well as the ligand-binding cavities has been proposed to mediate the enthalpy−entropy compensation effect in the overall binding processes.[53,76,77]

Recently, Portman et al. reported an enthalpy−entropy compensation effect for the binding γ-lactones to OBP3.[78] These authors argued that the molecular origin of the enthalpy−entropy compensation effect lies in the opposite thermodynamic signatures for the desolvation of the ligand surface and the binding cavity.[78] The desolvation of ligand surface (prior to its binding to protein) is analogous to the transfer of a nonpolar molecule from water to the nonpolar solvent, as previously suggested by Kauzmann, and thus, it contains the thermodynamic signatures of $+\Delta S$ and $+\Delta H$.[72] Contrastingly, the desolvation of the protein cavity releases the "high-energy" water molecule to the bulk solvent, yielding thermodynamic signatures of $-\Delta S$ and $-\Delta H$. Because the thermodynamic signatures for the desolvation of ligand and the binding cavity are opposite, they compensate for each other, leading to the enthalpy−entropy compensation effect. Notably, the aforementioned water-centric enthalpy−entropy compensation feature primarily relies on the fact that the water molecules surrounding the surface of the binding cavity are highly disordered. They make more hydrogen bonds ($-\Delta H$) with the surrounding water molecules and become more ordered ($-\Delta S$) upon being released to the bulk water. On the other hand, Klebe, Whitesides, and others have argued that the thermodynamic signatures for the release of water molecules from proteins' cavities (to the bulk phase) are dependent on the molecular contexts, i.e., their resident sites as well as the extent (partially or fully) to which they are ordered on the interacting surfaces.[73,76,79] Besides these water-centric views, Williams and co-workers maintain that the thermodynamic parameters derived from the binding of ligands to proteins cannot be easily explained in light of the local (interfacial) interactions because they are the property of the "whole" system.[60] For example, a remarkably tight binding affinity of biotin for streptavidin ($K_a = 10^{13}$ M^{-1}) cannot be rationalized on the basis of the interfacial forces between the interacting species.[60] In this regard, it is noteworthy that even a small (~1%) change in the hydrogen bonds in protein structures, mediated via the changes in the conformational flexibility of

dx.doi.org/10.1021/bi500711x | Biochemistry 2014, 53, 7445−7458

proteins upon the binding to their cognate ligands, contributes significantly to the overall thermodynamic parameters of the protein−ligand complexes.[60] Fenley et al. maintain that the ligand-assisted shift in the protein conformation plays a major role in the enthalpy−entropy compensation effect.[80] According to these authors, if the enthalpically driven ligand binding shifts the conformation of a protein from the "low entropic" state to the "high entropic" state, the enthalpic gain (due to ligand binding) will be essentially transduced (compensated) into the entropic changes in the protein structure.[80] Furthermore, the magnitude or extent of the conformational changes, contributing to the enthalpy−entropy compensation, will be dependent on the intrinsic dynamics of free and ligand-bound protein structures.[81,82] In view of these literature precedents, we conclude that the origin of the enthalpy−entropy compensation effect for the binding of the structural analogues of SAHA to HDAC8 lies both in the reorganization of water molecules and in the conformational flexibility in the enzyme structure. The latter feature is further evident from a remarkable difference in the crystallographically derived *B* factors of the apo and ligand-bound forms of HDAC8 (Figure S22 of the Supporting Information). Nonetheless, a thorough elucidation of the conformational flexibility and/or dynamics of HDAC8 in the presence of structurally diverse ligands must await high-resolution NMR studies.

In view of the observed thermodynamic parameters for the binding of different SAHA analogues to HDAC8, we argue that the different (i.e., "metal-binding", "linker", and "cap") regions of SAHA analogues interact differently with their complementary sites/regions at the active site of the enzyme, and the overall binding process is mediated both via local and global changes in protein conformation. Hence, the marked differences in the ligand-induced conformational changes in the enzyme even due to the structurally similar ligands, which may or may not be discernible via X-ray crystallography, would yield markedly different thermodynamic signatures for ligand binding. Given these, we conclude that the structure-based rational design of highly potent and/or isozyme-selective inhibitors of HDAC8 would be a challenging task. However, we believe that the inhibitory potency as well as the isozyme selectivity of a canonical HDAC inhibitor (e.g., SAHA) toward HDAC8 could be enhanced by attaching a "teether" moiety that could interact with the surface residues of the enzyme, akin to our "two-prong inhibitor design approach".[83,84] The "two-prong" approach to designing HDAC8 inhibitors appears to be logical considering that an extended peptide substrate binds to the enzyme's surface (designated as "exosites"), and such binding enhances the catalytic efficiency of the enzyme.[85] We are in the process of employing our two-prong inhibitor design strategy (by incorporating the "exosite" binding feature) to produce highly potent and HDAC8-selective inhibitors, and we will report these findings subsequently.

■ ASSOCIATED CONTENT

Supporting Information

Raw thermodynamic data and their fitted curves for the binding of all the SAHA analogues. This material is available free of charge via the Internet at http://pubs.acs.org.

■ AUTHOR INFORMATION

Corresponding Authors

*E-mail: raushan.singh@ndsu.edu.

*E-mail: dk.srivastava@ndsu.edu.

Funding

The research was supported by National Institutes of Health (NIH) Grant CA113746 and National Science Foundation Grant DMR 1306154 to D.K.S. and S.M. and NIH COBRE Grant NCRR-P20-RR15566 to G.C.

Notes

The authors declare no competing financial interest.

■ ACKNOWLEDGMENTS

We acknowledge the members of our research group for their valuable comments on the manuscript.

■ REFERENCES

(1) Fersht, A. (1998) *Structure and Mechanism in Protein Science: A Guide to Enzyme Catalysis and Protein Folding*, 1st ed., W. H. Freeman and Co., New York.

(2) Dembowsky, K., and Stadler, P. (2001) *Novel Therapeutic Proteins: Selected Case Studies*, 1st ed., Wiley-Blackwell, Hoboken, NJ.

(3) Ladbury, J. E., and Connelly, P. R. (1997) *Structure-Based Drug Design: Thermodynamics, Modeling, and Strategy (Biotechnology Intelligence Unit)*, 1st ed., R. G. Landes Co., Georgetown, TX.

(4) Teague, S. J. (2003) Implications of protein flexibility for drug discovery. *Nat. Rev. Drug Discovery 2*, 527−541.

(5) Davis, A. M., Teague, S. J., and Kleywegt, G. J. (2003) Application and limitations of X-ray crystallographic data in structure-based ligand and drug design. *Angew. Chem., Int. Ed. 42*, 2718−2736.

(6) Mobley, D. L., and Dill, K. A. (2009) Binding of Small-Molecule Ligands to Proteins: "What You See" Is Not Always "What You Get. *Structure 17*, 489−498.

(7) Somoza, J. R., Skene, R. J., Katz, B. A., Mol, C., Ho, J. D., Jennings, A. J., Luong, C., Arvai, A., Buggy, J. J., Chi, E., Tang, J., Sang, B.-C., Verner, E., Wynands, R., Leahy, E. M., Dougan, D. R., Snell, G., Navre, M., Knuth, M. W., Swanson, R. V., McRee, D. E., and Tari, L. W. (2004) Structural Snapshots of Human HDAC8 Provide Insights into the Class I Histone Deacetylases. *Structure 12*, 1325−1334.

(8) Dowling, D. P., Gantt, S. L., Gattis, S. G., Fierke, C. A., and Christianson, D. W. (2008) Structural studies of human histone deacetylase 8 and its site-specific variants complexed with substrate and inhibitors. *Biochemistry 47*, 13554−13563.

(9) Vannini, A., Volpari, C., Gallinari, P., Jones, P., Mattu, M., Carfí, A., De Francesco, R., Steinkühler, C., and Di Marco, S. (2007) Substrate binding to histone deacetylases as shown by the crystal structure of the HDAC8-substrate complex. *EMBO Rep. 8*, 879−884.

(10) Bradner, J. E., West, N., Grachan, M. L., Greenberg, E. F., Haggarty, S. J., Warnow, T., and Mazitschek, R. (2010) Chemical phylogenetics of histone deacetylases. *Nat. Chem. Biol. 6*, 238−243.

(11) Schultz, B. E., Misialek, S., Wu, J., Tang, J., Conn, M. T., Tahilramani, R., and Wong, L. (2004) Kinetics and Comparative Reactivity of Human Class I and Class IIb Histone Deacetylases. *Biochemistry 43*, 11083−11091.

(12) Wolfson, N. A., Pitcairn, C. A., and Fierke, C. A. (2013) HDAC8 substrates: Histones and beyond. *Biopolymers 99*, 112−126.

(13) De Ruijter, A. J. M., van Gennip, A. H., Caron, H. N., Kemp, S., and van Kuilenburg, A. B. P. (2003) Histone deacetylases (HDACs): Characterization of the classical HDAC family. *Biochem. J. 370*, 737−749.

(14) Choudhary, C., Kumar, C., Gnad, F., Nielsen, M. L., Rehman, M., Walther, T. C., Olsen, J. V., and Mann, M. (2009) Lysine acetylation targets protein complexes and co-regulates major cellular functions. *Science 325*, 834−840.

(15) Gregoretti, I. V., Lee, Y.-M., and Goodson, H. V. (2004) Molecular evolution of the histone deacetylase family: Functional implications of phylogenetic analysis. *J. Mol. Biol. 338*, 17−31.

(16) Blander, G., and Guarente, L. (2004) The Sir2 family of protein deacetylases. *Annu. Rev. Biochem. 73*, 417−435.

(17) Gao, L., Cueto, M. A., Asselbergs, F., and Atadja, P. (2002) Cloning and functional characterization of HDAC11, a novel member

of the human histone deacetylase family. *J. Biol. Chem. 277*, 25748−25755.
(18) Gallinari, P., Di Marco, S., Jones, P., Pallaoro, M., and Steinkühler, C. (2007) HDACs, histone deacetylation and gene transcription: From molecular biology to cancer therapeutics. *Cell Res. 17*, 195−211.
(19) Oehme, I., Deubzer, H. E., Wegener, D., Pickert, D., Linke, J.-P., Hero, B., Kopp-Schneider, A., Westermann, F., Ulrich, S. M., von Deimling, A., Fischer, M., and Witt, O. (2009) Histone deacetylase 8 in neuroblastoma tumorigenesis. *Clin. Cancer Res. 15*, 91−99.
(20) Maris, J. M., Hogarty, M. D., Bagatell, R., and Cohn, S. L. (2007) Neuroblastoma. *Lancet 369*, 2106−2120.
(21) Chuang, D.-M., Leng, Y., Marinova, Z., Kim, H.-J., and Chiu, C.-T. (2009) Multiple roles of HDAC inhibition in neurodegenerative conditions. *Trends Neurosci. 32*, 591−601.
(22) Deardorff, M. A., Bando, M., Nakato, R., Watrin, E., Itoh, T., Minamino, M., Saitoh, K., Komata, M., Katou, Y., Clark, D., Cole, K. E., De Baere, E., Decroos, C., Di Donato, N., Ernst, S., Francey, L. J., Gyftodimou, Y., Hirashima, K., Hullings, M., Ishikawa, Y., Jaulin, C., Kaur, M., Kiyono, T., Lombardi, P. M., Magnaghi-Jaulin, L., Mortier, G. R., Nozaki, N., Petersen, M. B., Seimiya, H., Siu, V. M., Suzuki, Y., Takagaki, K., Wilde, J. J., Willems, P. J., Prigent, C., Gillessen-Kaesbach, G., Christianson, D. W., Kaiser, F. J., Jackson, L. G., Hirota, T., Krantz, I. D., and Shirahige, K. (2012) HDAC8 mutations in Cornelia de Lange syndrome affect the cohesin acetylation cycle. *Nature 489*, 313−317.
(23) Bolden, J. E., Peart, M. J., and Johnstone, R. W. (2006) Anticancer activities of histone deacetylase inhibitors. *Nat. Rev. Drug Discovery 5*, 769−784.
(24) Wagner, J. M., Hackanson, B., Lubbert, M., and Jung, M. (2010) Histone deacetylase (HDAC) inhibitors in recent clinical trials for cancer therapy. *Clin. Epigenet. 1*, 117−136.
(25) Hu, E., Dul, E., Sung, C.-M., Chen, Z., Kirkpatrick, R., Zhang, G.-F., Johanson, K., Liu, R., Lago, A., Hofmann, G., Macarron, R., de los Frailes, M., Perez, P., Krawiec, J., Winkler, J., and Jaye, M. (2003) Identification of novel isoform-selective inhibitors within class I histone deacetylases. *J. Pharmacol. Exp. Ther. 307*, 720−728.
(26) Krennhrubec, K., Marshall, B. L., Hedglin, M., Verdin, E., and Ulrich, S. M. (2007) Design and evaluation of "linkerless" hydroxamic acids as selective HDAC8 inhibitors. *Bioorg. Med. Chem. Lett. 17*, 2874−2878.
(27) Galletti, P., Quintavalla, A., Ventrici, C., Giannini, G., Cabri, W., Penco, S., Gallo, G., Vincenti, S., and Giacomini, D. (2009) Azetidinones as zinc-binding groups to design selective HDAC8 inhibitors. *ChemMedChem 4*, 1991−2001.
(28) Garbett, N. C., and Chaires, J. B. (2012) Thermodynamic studies for drug design and screening. *Expert Opin. Drug Discovery 7*, 299−314.
(29) Freire, E. (2008) Do enthalpy and entropy distinguish first in class from best in class? *Drug Discovery Today 13*, 869−874.
(30) Ladbury, J. E., Klebe, G., and Freire, E. (2010) Adding calorimetric data to decision making in lead discovery: A hot tip. *Nat. Rev. Drug Discovery 9*, 23−27.
(31) Olsson, T. S. G., Williams, M. A., Pitt, W. R., and Ladbury, J. E. (2008) The Thermodynamics of Protein−Ligand Interaction and Solvation: Insights for Ligand Design. *J. Mol. Biol. 384*, 1002−1017.
(32) Schön, A., Madani, N., Smith, A. B., Lalonde, J. M., and Freire, E. (2011) Some binding-related drug properties are dependent on thermodynamic signature. *Chem. Biol. Drug Des. 77*, 161−165.
(33) Bantscheff, M., Hopf, C., Savitski, M. M., Dittmann, A., Grandi, P., Michon, A.-M., Schlegl, J., Abraham, Y., Becher, I., Bergamini, G., Boesche, M., Delling, M., Dümpelfeld, B., Eberhard, D., Huthmacher, C., Mathieson, T., Poeckel, D., Reader, V., Strunk, K., Sweetman, G., Kruse, U., Neubauer, G., Ramsden, N. G., and Drewes, G. (2011) Chemoproteomics profiling of HDAC inhibitors reveals selective targeting of HDAC complexes. *Nat. Biotechnol. 29*, 255−265.
(34) Singh, R. K., Mandal, T., Balasubramanian, N., Cook, G., and Srivastava, D. K. (2011) Coumarin-suberoylanilide hydroxamic acid as a fluorescent probe for determining binding affinities and off-rates of histone deacetylase inhibitors. *Anal. Biochem. 408*, 309−315.
(35) Suzuki, T., Kouketsu, A., Matsuura, A., Kohara, A., Ninomiya, S.-I., Kohda, K., and Miyata, N. (2004) Thiol-based SAHA analogues as potent histone deacetylase inhibitors. *Bioorg. Med. Chem. Lett. 14*, 3313−3317.
(36) Gediya, L. K., Chopra, P., Purushottamachar, P., Maheshwari, N., and Njar, V. C. O. (2005) A New Simple and High-Yield Synthesis of Suberoylanilide Hydroxamic Acid and Its Inhibitory Effect Alone or in Combination with Retinoids on Proliferation of Human Prostate Cancer Cells. *J. Med. Chem. 48*, 5047−5051.
(37) Tellinghuisen, J., and Chodera, J. D. (2011) Systematic errors in isothermal titration calorimetry: Concentrations and baselines. *Anal. Biochem. 414*, 297−299.
(38) Wiseman, T., Williston, S., Brandts, J. F., and Lin, L. N. (1989) Rapid measurement of binding constants and heats of binding using a new titration calorimeter. *Anal. Biochem. 179*, 131−137.
(39) Goldberg, R. N., Kishore, N., and Lennen, R. M. (2002) Thermodynamic quantities for the ionization reactions of buffers. *J. Phys. Chem. Ref. Data 31*, 231−370.
(40) Fraczkiewicz, R., and Braun, W. (1998) Exact and efficient analytical calculation of the accessible surface areas and their gradients for macromolecules. *J. Comput. Chem. 19*, 319−333.
(41) Murphy, K. P., and Freire, E. (1992) Thermodynamics of structural stability and cooperative folding behavior in proteins. *Adv. Protein Chem. 43*, 313−361.
(42) Baker, B. M., and Murphy, K. P. (1996) Evaluation of linked protonation effects in protein binding reactions using isothermal titration calorimetry. *Biophys. J. 71*, 2049−2055.
(43) Parker, M. H., Lunney, E. A., Ortwine, D. F., Pavlovsky, A. G., Humblet, C., and Brouillette, C. G. (1999) Analysis of the binding of hydroxamic acid and carboxylic acid inhibitors to the stromelysin-1 (matrix metalloproteinase-3) catalytic domain by isothermal titration calorimetry. *Biochemistry 38*, 13592−13601.
(44) Chiu, Y.-H., Gabriel, G. J., and Canary, J. W. (2005) Ternary ligand-zinc-hydroxamate complexes. *Inorg. Chem. 44*, 40−44.
(45) Hansen, R. E., and Winther, J. R. (2009) An introduction to methods for analyzing thiols and disulfides: Reactions, reagents, and practical considerations. *Anal. Biochem. 394*, 147−158.
(46) Wu, R., Lu, Z., Cao, Z., and Zhang, Y. (2011) Zinc chelation with hydroxamate in histone deacetylases modulated by water access to the linker binding channel. *J. Am. Chem. Soc. 133*, 6110−6113.
(47) Chen, K., Zhang, X., Wu, Y.-D., and Wiest, O. (2014) Inhibition and Mechanism of HDAC8 Revisited. *J. Am. Chem. Soc. 136*, 11636−11643.
(48) Baldwin, R. L. (1986) Temperature dependence of the hydrophobic interaction in protein folding. *Proc. Natl. Acad. Sci. U.S.A. 83*, 8069−8072.
(49) Privalov, P. L., and Makhatadze, G. I. (1990) Heat capacity of proteins. II. Partial molar heat capacity of the unfolded polypeptide chain of proteins: Protein unfolding effects. *J. Mol. Biol. 213*, 385−391.
(50) Loladze, V. V., Ermolenko, D. N., and Makhatadze, G. I. (2001) Heat capacity changes upon burial of polar and nonpolar groups in proteins. *Protein Sci. 10*, 1343−1352.
(51) Syme, N. R., Dennis, C., Phillips, S. E. V., and Homans, S. W. (2007) Origin of Heat Capacity Changes in a "Nonclassical" Hydrophobic Interaction. *ChemBioChem 8*, 1509−1511.
(52) Dunitz, J. D. (1995) Win some, lose some: Enthalpy-entropy compensation in weak intermolecular interactions. *Chem. Biol. 2*, 709−712.
(53) Lumry, R., and Rajender, S. (1970) Enthalpy-entropy compensation phenomena in water solutions of proteins and small molecules: A ubiquitous property of water. *Biopolymers 9*, 1125−1227.
(54) Lumry, R. (2003) Uses of enthalpy-entropy compensation in protein research. *Biophys. Chem. 105*, 545−557.
(55) Lumry, R. (2003) Practical limitations on the use of thermodynamic data from isothermal processes. *Biophys. Chem. 105*, 609−620.

(56) Gurard-Levin, Z. A., Kim, J., and Mrksich, M. (2009) Combining mass spectrometry and peptide arrays to profile the specificities of histone deacetylases. *ChemBioChem 10*, 2159−2161.
(57) Watkins, R. E., Wisely, G. B., Moore, L. B., Collins, J. L., Lambert, M. H., Williams, S. P., Willson, T. M., Kliewer, S. A., and Redinbo, M. R. (2001) The human nuclear xenobiotic receptor PXR: Structural determinants of directed promiscuity. *Science 292*, 2329−2333.
(58) Redinbo, M. R. (2004) Promiscuity: What protects us, perplexes us. *Drug Discovery Today 9*, 431−432.
(59) Khersonsky, O., and Tawfik, D. S. (2010) Enzyme promiscuity: A mechanistic and evolutionary perspective. *Annu. Rev. Biochem. 79*, 471−505.
(60) Williams, D. H., Stephens, E., O'Brien, D. P., and Zhou, M. (2004) Understanding noncovalent interactions: Ligand binding energy and catalytic efficiency from ligand-induced reductions in motion within receptors and enzymes. *Angew. Chem., Int. Ed. 43*, 6596−6616.
(61) Christensen, T., Gooden, D. M., Kung, J. E., and Toone, E. J. (2003) Additivity and the physical basis of multivalency effects: A thermodynamic investigation of the calcium EDTA interaction. *J. Am. Chem. Soc. 125*, 7357−7366.
(62) Lowther, W. T., and Matthews, B. W. (2000) Structure and function of the methionine aminopeptidases. *Biochim. Biophys. Acta 1477*, 157−167.
(63) Rajagopalan, P. T. R., Grimme, S., and Pei, D. (2000) Characterization of Cobalt(II)-Substituted Peptide Deformylase: Function of the Metal Ion and the Catalytic Residue Glu-133. *Biochemistry 39*, 779−790.
(64) Srivastava, D. K., Wang, S., and Peterson, K. L. (1997) Isothermal titration microcalorimetric studies for the binding of octenoyl-CoA to medium chain acyl-CoA dehydrogenase. *Biochemistry 36*, 6359−6366.
(65) Cooper, A. (1999) Thermodynamic analysis of biomolecular interactions. *Curr. Opin. Chem. Biol. 3*, 557−563.
(66) Chodera, J. D., and Mobley, D. L. (2013) Entropy-enthalpy compensation: Role and ramifications in biomolecular ligand recognition and design. *Annu. Rev. Biophys. 42*, 121−142.
(67) Singh, R. K., Lall, N., Leedahl, T. S., McGillivray, A., Mandal, T., Haldar, M., Mallik, S., Cook, G., and Srivastava, D. K. (2013) Kinetic and Thermodynamic Rationale for Suberoylanilide Hydroxamic Acid Being a Preferential Human Histone Deacetylase 8 Inhibitor As Compared to the Structurally Similar Ligand, Trichostatin A. *Biochemistry 52*, 8139−8149.
(68) Lumry, R., and Eyring, H. (1954) Conformation Changes of Proteins. *J. Phys. Chem. 58*, 110−120.
(69) Berg, A. K., and Srivastava, D. K. (2009) Delineation of alternative conformational states in *Escherichia coli* peptide deformylase via thermodynamic studies for the binding of actinonin. *Biochemistry 48*, 1584−1594.
(70) Gallicchio, E., Kubo, M. M., and Levy, R. M. (1998) Entropy−Enthalpy Compensation in Solvation and Ligand Binding Revisited. *J. Am. Chem. Soc. 120*, 4526−4527.
(71) Sharp, K. (2001) Entropy−enthalpy compensation: Fact or artifact? *Protein Sci. 10*, 661−667.
(72) Kauzmann, W. (1959) Some factors in the interpretation of protein denaturation. *Adv. Protein Chem. 14*, 1−63.
(73) Snyder, P. W., Mecinovic, J., Moustakas, D. T., Thomas, S. W., Harder, M., Mack, E. T., Lockett, M. R., Héroux, A., Sherman, W., and Whitesides, G. M. (2011) Mechanism of the hydrophobic effect in the biomolecular recognition of arylsulfonamides by carbonic anhydrase. *Proc. Natl. Acad. Sci. U.S.A. 108*, 17889−17894.
(74) Lafont, V., Armstrong, A. A., Ohtaka, H., Kiso, Y., Mario Amzel, L., and Freire, E. (2007) Compensating Enthalpic and Entropic Changes Hinder Binding Affinity Optimization. *Chem. Biol. Drug Des. 69*, 413−422.
(75) Qian, H. (1998) Entropy-enthalpy compensation: Conformational fluctuation and induced-fit. *J. Chem. Phys. 109*, 10015−10017.
(76) Breiten, B., Lockett, M. R., Sherman, W., Fujita, S., Al-Sayah, M., Lange, H., Bowers, C. M., Heroux, A., Krilov, G., and Whitesides, G. M. (2013) Water Networks Contribute to Enthalpy/Entropy Compensation in Protein−Ligand Binding. *J. Am. Chem. Soc. 135*, 15579−15584.
(77) Grunwald, E., and Steel, C. (1995) Solvent Reorganization and Thermodynamic Enthalpy-Entropy Compensation. *J. Am. Chem. Soc. 117*, 5687−5692.
(78) Portman, K. L., Long, J., Carr, S., Briand, L., Winzor, D. J., Searle, M. S., and Scott, D. J. (2014) Enthalpy/Entropy Compensation Effects from Cavity Desolvation Underpin Broad Ligand Binding Selectivity for Rat Odorant Binding Protein 3. *Biochemistry 53*, 2371−2379.
(79) Biela, A., Nasief, N. N., Betz, M., Heine, A., Hangauer, D., and Klebe, G. (2013) Dissecting the hydrophobic effect on the molecular level: The role of water, enthalpy, and entropy in ligand binding to thermolysin. *Angew. Chem., Int. Ed. 52*, 1822−1828.
(80) Fenley, A. T., Muddana, H. S., and Gilson, M. K. (2012) Entropy-enthalpy transduction caused by conformational shifts can obscure the forces driving protein-ligand binding. *Proc. Natl. Acad. Sci. U.S.A. 109*, 20006−20011.
(81) Diehl, C., Engström, O., Delaine, T., Håkansson, M., Genheden, S., Modig, K., Leffler, H., Ryde, U., Nilsson, U. J., and Akke, M. (2010) Protein Flexibility and Conformational Entropy in Ligand Design Targeting the Carbohydrate Recognition Domain of Galectin-3. *J. Am. Chem. Soc. 132*, 14577−14589.
(82) Ferrante, A., and Gorski, J. (2012) Enthalpy-entropy compensation and cooperativity as thermodynamic epiphenomena of structural flexibility in ligand-receptor interactions. *J. Mol. Biol. 417*, 454−467.
(83) Banerjee, A. L., Eiler, D., Roy, B. C., Jia, X., Haldar, M. K., Mallik, S., and Srivastava, D. K. (2005) Spacer-based selectivity in the binding of "two-prong" ligands to recombinant human carbonic anhydrase I. *Biochemistry 44*, 3211−3224.
(84) Jude, K. M., Banerjee, A. L., Haldar, M. K., Manokaran, S., Roy, B., Mallik, S., Srivastava, D. K., and Christianson, D. W. (2006) Ultrahigh resolution crystal structures of human carbonic anhydrases I and II complexed with "two-prong" inhibitors reveal the molecular basis of high affinity. *J. Am. Chem. Soc. 128*, 3011−3018.
(85) Gurard-Levin, Z. A., and Mrksich, M. (2008) The activity of HDAC8 depends on local and distal sequences of its peptide substrates. *Biochemistry 47*, 6242−6250.